Stereodynamics of Bond Rotation in Tertiary Aromatic Amides

Ryan A. Bragg, Jonathan Clayden,* Gareth A. Morris, and Jennifer H. Pink[a]

Abstract: The degree to which the rotations about the C–N and Ar–CO bonds of aromatic amides occur in a concerted manner was investigated by a variety of NMR and kinetic techniques. Otherwise complex kinetic analyses were simplified by exploiting symmetry and asymmetry in the N-substituents of amides. In 2-unsubstituted 1-naphthamides bearing branched N-substituents, most conformational changes about the amide group were by correlated rotation, though uncorrelated Ar–CO rotation also occurred to some extent. In 2-substituted 1-naphthamides, correlated rotation accounted for all of the Ar–CO rotations, though a significant amount of uncorrelated C–N rotation also occurred. Naphthamides bearing branched N-substituents thus turn out to be efficient molecular gears: Com-

Keywords: amides · bond rotation · NMR spectroscopy · saturation transfer

Introduction

Tertiary aromatic amides **1** are not in general planar, and even moderate steric hindrance forces a dihedral angle of 90° on the Ar–CO bond.[1] Subject to certain constraints of substitution pattern (such as X ≠ Y), the two perpendicular conformers about the Ar–CO bond are enantiomeric, and when the rate of rotation about this bond is slow the compound **1** is atropisomeric.[2, 3] For simple amides **1** bearing achiral substituents X, Y and R, the rate of rotation about the Ar–CO bond is also the rate of enantiomerisation (half the rate of racemisation). We[4, 5] and others[6–11] have determined the rates of enantiomerisation of a range of amides **1**: As a rule, 2,6-disubstituted tertiary benzamides (and 2-substituted naphthamides) are atropisomeric at ambient temperatures (half-life for racemisation greater than an arbitrary 1000 s[12]) but 2-substituted benzamides are not.

For more complex amides bearing chiral substituents R, X or Y, the conformers about Ar–CO are diastereoisomeric, and at equilibrium they need not be equally populated. We have exploited examples with chiral X and Y in which one conformer is heavily favoured over the other to transfer stereochemistry from a stereogenic centre attached to the aromatic ring to the stereogenic axis of the amide.[13–20]

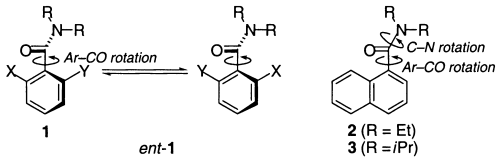

For the more rapidly rotating (non-atropisomeric) amides, we have followed[4] the interconversion of diastereotopic ^{1}H NMR signals by variable temperature nuclear magnetic resonance (VT NMR) techniques,[21] being aware nonetheless of their limitations.[22, 23] We were able in some cases to observe not only coalescence of peaks arising from the slow Ar–CO rotations but also coalescence of peaks arising from slow C–N rotation.[24] This enabled us to estimate also the rate of rotation about the C–N bond of some of the compounds. We found that, for less hindered amides (up to and including **2** for example), C–N rotation occurs rather more slowly than Ar–CO rotation, but that as steric hindrance increases, the rate of Ar–CO rotation decreases until, in the most hindered example we studied, **3**, the two appear to have about the same rate. This led us to speculate at that time that Ar–CO rotation may be correlated with C–N rotation: the two rotations may not be occurring independently but as a single geared (concerted) process. Similar correlated rotations in amides,[10] diamides[25] and thioamides[26, 27] have been previously proposed, but lack of symmetry in the molecules under investigation led to complex kinetic schemes involving numerous unrelated rate constants. In this paper we present in full our use of symmetrical amides to simplify the analysis of the kinetics of correlated rotation, and we conclude that geared bond rotation is a common feature of hindered aromatic amides.[28, 29]

[a] Prof. J. Clayden, R. A. Bragg, Prof. G. A. Morris, Dr. J. H. Pink
Department of Chemistry
University of Manchester, Oxford Road
Manchester M13 9PL (UK)
Fax: (+44) 161-275-4939
E-mail: j.p.clayden@man.ac.uk

Supporting information for this article is available on the WWW under http://www.wiley-vch.de/home/chemistry/ or from the author.

  0947-6539/02/0806-1279 $ 17.50+.50/0

VT NMR experiments on tertiary amides with one chiral N-substituent: We started with a set of amides in which all four possible rotamers arising from Ar–CO and C–N rotation are diastereoisomeric, unlike **1**–**3**. The amides **4**–**9** were made by acylation of the amines with 1-naphthoyl chloride (benzoyl chloride for **8**). The diastereoisomeric conformers of

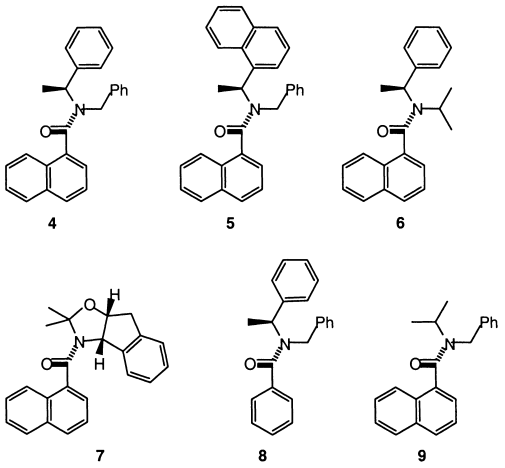

these compounds interconvert by rotation about their Ar–CO and C–N bonds sufficiently slowly for them to give rise to clear, discrete sets of signals in their NMR spectra at room temperature or just below. For each compound, four diastereoisomeric conformers were discernible, divided into one more populated pair and one less populated pair, with ratios shown in Table 1 and tentatively assigned structures in Scheme 1. We assume the significant population difference *between* the pairs arises from their being different C–N rotamers (*cis* or *trans*); the small population difference *within* each pair arises from their being different Ar–CO conformers (*M* and *P*). This analysis is supported by the populations of the two conformers of **8** and **9**, which can exhibit only *cis*/*trans* rotamers; the ratio of 3:1 approximates to the *cis*/*trans* ratio of the similar compound **4**. By integration it was therefore straightforward to make provisional assignments of the peaks in the spectrum to the four conformers.

Table 1. Populations of diastereoisomeric conformers of amides **4**–**9**.

	Compound	Solvent, T [°C]	(*P*, *cis*)	(*M*, *cis*)	(*P*, *trans*)	(*M*, *trans*)
1	**4**	$CDCl_3$, –20	0.19	0.12	0.33	0.35
2	**5**	$CDCl_3$, –20	0.47	0.47	0.04	0.02
3	**6**	$CDCl_3$, –20	0.10	0.10	0.41	0.39
4	**7**	$CDCl_3$, –55	0.63	0.24	0.09	0.04
5	**8**	$CDCl_3$, –20	0.25	–	0.75	–
6	**9**	$CDCl_3$, –20	0.25	–	0.75	–

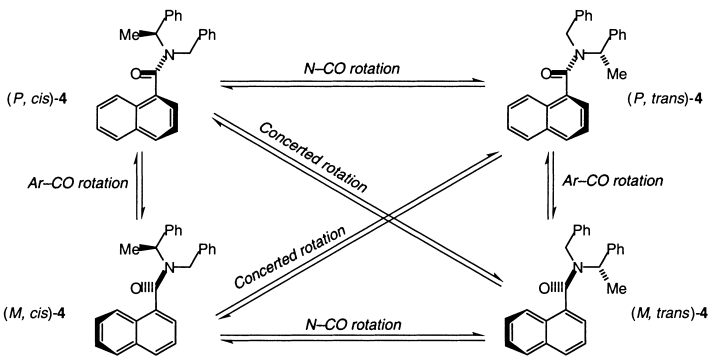

Scheme 1. Conformational interconversions in **4**.

Assignment of stereochemistry to the conformers is tentative: The *cis*/*trans* assignment is based on the expectation that signals of N-substituents *cis* to O are shifted downfield relative to those of N-substituents *cis* to the aromatic ring.[4, 30] The surprising preference of **4**, **6**, **8** and **9** for what appears to be the more crowded amide geometry is precedented,[30, 31] and the similarity of the spectra of **4** and **5** allows us reasonable confidence in assigning them opposite preferred amide geometry. The *M*/*P* assignment is purely arbitrary, though we chose to assign (*M*, *trans*) to the major conformer of **4** and (*P*, *cis*) stereochemistry to the major conformer of **7** as these are the conformations adopted in the crystalline state (see Figure 1).[32]

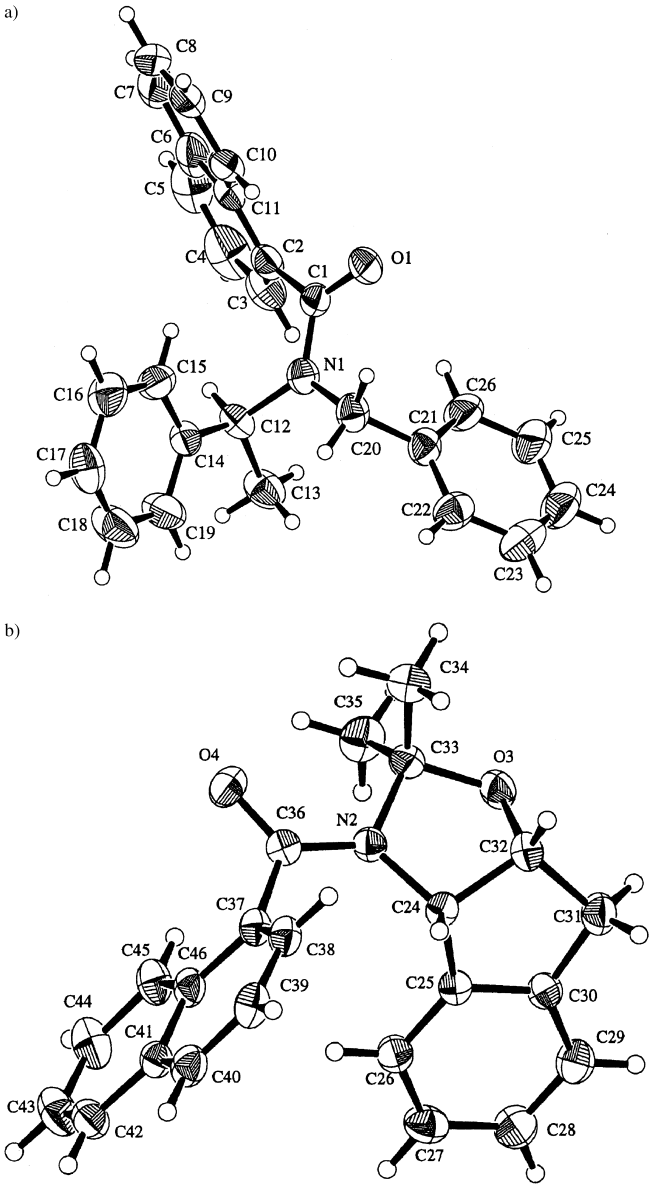

Figure 1. a) X-ray crystal structure of **4** [showing (*M*, *trans*) conformation]; b) X-ray crystal structure of **7** [showing (*P*, *cis*) conformation].

0947-6539/02/0806-1280 $ 17.50+.50/0 *Chem. Eur. J.* **2002**, *8*, No. 6

We had hoped that VT NMR studies of amides **4**–**7** would allow us to follow the interconversion of the rotamers in detail by analysing the patterns of coalescence between various pairs of signals, and variable temperature NMR experiments with **4**–**7** were carried out in $CDCl_3$ or [D_6]DMSO at 300 MHz. In the event, ^{1}H NMR spectra acquired at increased temperatures led to very complex, broadened lineshapes from which it was possible to draw only the most general of conclusions. Figure 2a shows how the lineshapes of signals corresponding to the methyl doublet of the conformers of **4** ($Me^{(M,\,cis)}$, $Me^{(M,\,trans)}$ etc.) change with increasing temperature. A simple qualitative conclusion is quite clear: The signals of the minor pair of conformers (*M*, *cis*) and (*P*, *cis*)-**4** coalesce well before the signals of the major pair of conformers (*M*, *trans*) and (*P*, *trans*)-**4**, despite having a greater chemical shift difference. A similar pattern was evident in other signals belonging to the four rotamers. Given the apparent isolation of the conformational process interconverting the (*M*, *cis*) and (*P*, *cis*) rotamers from interconversions of the (*M*, *trans*) and (*P*, *trans*) rotamers or from interconversion of *cis* and *trans*, we applied the Gutowski–Holm equations to these signals (which show only a moderate population bias)[21] to obtain a crude estimate of the rate of Ar–CO rotation in the *cis* rotamers. Table 2, entries 1–3, tabulates the chemical shift differences between the H_{Me}, H_q and H_{Ar} signals in the *M* and *P* rotamers of the *cis* conformer, their coalescence temperatures, and estimates of *k* (the rate constant for conformational interconversion, i.e., Ar–CO rotation), $\Delta G^{\ddagger}$ (the barrier to Ar–CO rotation), and $t_{1/2}$ (the half-life for Ar–CO rotation at 20 °C, assuming $\Delta G^{\ddagger}$ is invariant with temperature). The three estimates of $\Delta G^{\ddagger}$ lie within experimental error, and are also close in value to the previously determined barrier to Ar–CO rotation in *N*,*N*-dibenzyl-1-naphthamide and in the minor conformer of *N*-benzyl-*N*-isopropyl-1-naphthamide *cis*-**9**.[4]

Analysis of the coalescence of signals for the major, *trans* conformer (Table 2, entry 4) gives a rather higher barrier to rotation from *M* to *P* about the Ar–CO bond, as would be expected. The figures obtained match those for other amides bearing branched substituents *trans* to O (and therefore close to the aromatic ring), including *N*,*N*-diisopropyl-1-naphthamide and the major conformer of *N*-benzyl-*N*-isopropyl-1-naphthamide *trans*-**9**.[4]

Conformational interconversion of the *trans* rotamers of **4** can be observed more clearly in DMSO at temperatures exceeding 50 °C (Table 2, entries 5, 6). The spectra of **4** in DMSO are shown in Figure 2b. At 20 °C in DMSO, coalescences of the signals for the *cis* isomer are well under way; broadening of the signals of the *trans* conformers begins at 40 °C and coalescence takes place at 81 °C. Tentative figures derived from these and other signals are given in Table 2. However, some of these coalescences appear to involve not only the *M* and *P* rotamers of the *trans* conformer, but also the already-coalesced signals arising from (*M*, *cis*) and (*P*, *cis*)-**4** (note too the way that, in Figure 2a, the $Me^{(M,\,trans)}$ signal closer to the coalesced *cis* signals broadens more than the $Me^{(P,\,trans)}$ signal further from them). Purely qualitatively, this suggests that while the less congested interconversion of (*M*, *cis*) and (*P*, *cis*)-**4** may take place without concerted rotation,

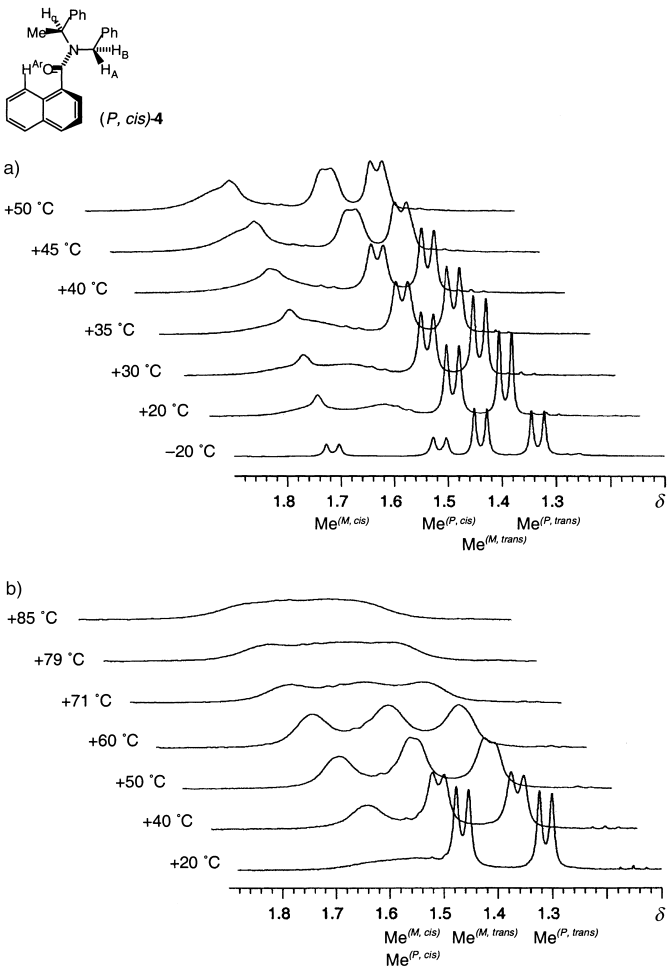

Figure 2. VT NMR of **4** in a) $CDCl_3$, b) [D_6]DMSO.

interconversion of the rotamers of *trans*-**4** may involve both Ar–CO and C–N rotation.

Amide **5** behaves similarly, with the signals of the *cis* isomer coalescing sooner than for the *trans* isomer. The major signals of **5** (assigned to *cis*-**5**) are broadened in $CDCl_3$ even at 20 °C and there is a clear coalescence of the major Me signals at 24 °C (Table 2, entry 7) corresponding to an approximate barrier again matching closely that of *cis*-**4** and of *N*,*N*-dibenzyl-1-naphthamide. The minor signals of **5** (assigned to *trans*-**5**) remain sharp to much higher temperatures, but we could draw no conclusions with regard to the concerted nature of the rotations.

Figure 3 shows a series of ^{1}H NMR spectra of the methyl singlet region of **7** in $CDCl_3$ at temperatures between −50 and +50 °C. Again, the signals of the *cis* isomer coalesce first, and in this case there is evidence that the resulting *cis* signals become involved in the coalescence of the signals of the *trans* isomer. The signals for the two $Me^{(P,\,cis)}$ signals coalesce with those of the $Me^{(M,\,cis)}$ at about −25 °C. Importantly, all four signals due to the *trans* isomer retain the same degree of broadening throughout this coalescence, and $Me_A^{(P,\,trans)}$ at about δ1.56 remains sharp despite its closeness to $Me_B^{(P,\,cis)}$; this indicates that Ar–CO rotation in the *cis* isomer is totally independent of C–N rotation. The coalescences of the *cis* signals correspond to a barrier to Ar–CO rotation of

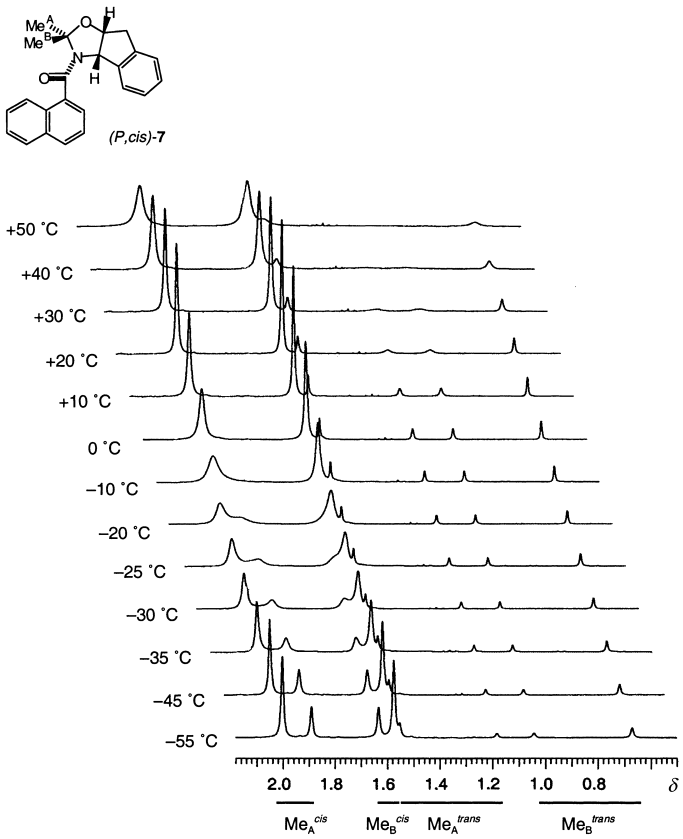

Figure 3. VT NMR of **7** in $CDCl_3$.

55 kJ mol^{-1} (Table 2, entries 8 and 9). By +10 °C, the *M* and *P* rotamers of the *cis* isomer no longer give rise to discrete signals, and single sharp Me_A^{cis} and Me_B^{cis} singlets are observed. At this temperature, coalescence of the signals due to the *trans* isomer of **7** begins. $Me_A^{(M,trans)}$ and $Me_B^{(M,trans)}$ begin to broaden at +20 °C, but these signals cannot be interconverting with each other because they are diastereotopic signals arising from the same conformer—the broadening arises from coalescences of $Me_A^{(M,trans)}$ with $Me_A^{(P,trans)}$ and of $Me_B^{(M,trans)}$ with $Me_B^{(P,trans)}$, and final coalescence must take place at >55 °C, as shown in Table 2, entry 10. However, it seems that Ar–CO rotation of the *trans* isomer of **7** is not fully independent of C–N rotation. During the coalescence of the *trans* peaks the newly sharpened *cis* peaks begin to broaden again; this suggests that Ar–CO rotation of the *trans* conformers involves interconversions with the *cis* conformers, and is to some extent correlated with C–N rotation.

The complexity of these systems, with at least six possible processes interconverting the rotamers of **4**, **5** and **7** meant that attempts at more detailed lineshape analysis of these coalescences were fruitless.

VT NMR experiments on tertiary amides with two chiral N-substituents: The three compounds **10**–**12** overcome some of the problems associated with the detailed analysis of **4**, **5** and **7** since symmetry means that they possess only two diastereoisomeric conformers, giving rise to only two sets of signals in the NMR spectra. All three were made by the methods described below (see Experimental Section), and their symmetry places them in two classes.

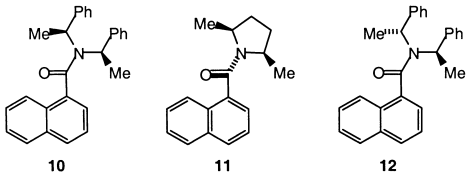

The *meso*-compounds **10** and **11** can exist as two diastereoisomeric conformers, which we name *exo* and *endo* according to the relationship between the Me group and the naphthalene ring. Either a C–N or an Ar–CO rotation will convert *exo* to *endo* or vice versa, as shown in Scheme 2. But there is a subtle difference between these two rotations: From any single conformer, both rotations give rise to its diastereoisomer, but Ar–CO rotation gives one enantiomer while C–N rotation gives the other. The overall effect of a concerted Ar–CO/C–N rotation however is merely enantiomerisation: *Concerted rotations do not interconvert diastereoisomeric conformers.*

The assignment of *endo* or *exo*, *cis* or *trans* to every peak in the NMR spectrum is in principle achievable by using integration (the ratio between the two diastereoisomeric conformers is close to, but not exactly, 1) and chemical shift (we expect the *cis* methyl groups to be upfield of the *trans*). However, it is possible to come to significant conclusions regarding the importance or otherwise of correlated rotations in these compounds even without detailed assignment of signals. Because both Ar–CO and C–N rotations exchange the signals of the two diastereoisomers, they must lead to an exchange involving every peak in the entire NMR spectrum of **10**. However, the correlated rotations, which interconvert the enantiomers of either the *exo* or the *endo* diastereoisomeric conformer, involve only the signals arising from that diastereoisomer, and furthermore interconvert only signals

Table 2. VT NMR studies of **4**, **5** and **7**.

Entry	Amide	Solvent	Coalescing signals	$\Delta\nu$ [Hz]	T_c [°C]	k [s^{-1}]	$\Delta G^{\ddagger}_{Ar-CO}$[a] [kJ mol^{-1}]	half-life[b] [s]
1	*cis*-**4**	$CDCl_3$	$Me^{(M,cis)}-Me^{(P,cis)}$	60	32	133	62.3	0.007
2	*cis*-**4**	$CDCl_3$	$H_q^{(M,cis)}-H_q^{(P,cis)}$	56	31	124	62.3	0.007
3	*cis*-**4**	$CDCl_3$	$H_{Ar}^{(M,cis)}-H_{Ar}^{(P,cis)}$	90	35	200	61.9	0.007
4	*trans*-**4**	$CDCl_3$	$H_{Ar}^{(M,trans)}-H_{Ar}^{(P,trans)}$	24	52	53	69.1	0.12
5	*trans*-**4**	DMSO	$Me^{(M,trans)}-Me^{(P,trans)}$	45	81	100	73.6	0.75
6	*trans*-**4**	DMSO	$H_q^{(M,trans)}$-$H_q^{(P,trans)}$	26	57	58	69.9	0.16
7	*cis*-**5**	$CDCl_3$	$Me^{(M,cis)}-Me^{(P,cis)}$	38	24	83	61.8	0.005
8	*cis*-**7**	$CDCl_3$	$Me_A^{(M,cis)}-Me_A^{(P,cis)}$	34	−20	24	55.0	0.0003
9	*cis*-**7**	$CDCl_3$	$Me_B^{(M,cis)}-Me_B^{(P,cis)}$	17	−30	8	54.9	0.0003
10	*trans*-**7**	$CDCl_3$	$Me_A^{(M,trans)}-Me_A^{(P,trans)}$	113	>55	100	>68	>0.7

[a] Value at coalescence temperature T_c; error ±1 kJ mol^{-1}. [b] Estimated half-life for racemisation at 20 °C, assuming constancy of $\Delta G^{\ddagger}_{Ar-CO}$ with temperature. Note that k is the rate of enantiomerisation of the amide; the rate of racemisation is $k/2$.

0947-6539/02/0806-1282 $ 17.50+.50/0 *Chem. Eur. J.* **2002**, *8*, No. 6

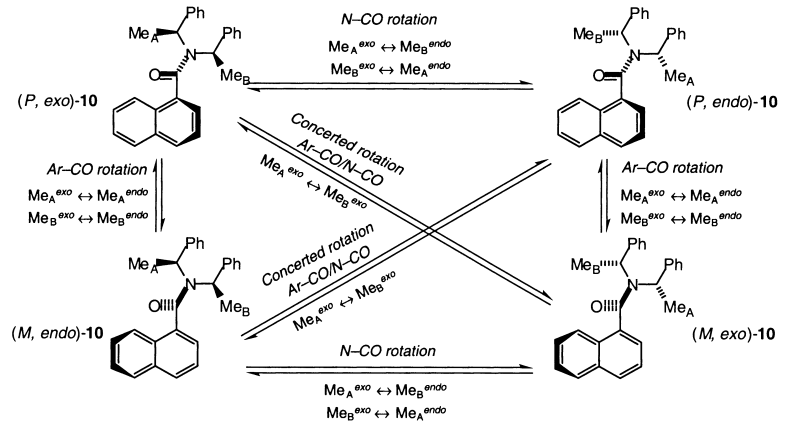

Scheme 2. Conformational interconversions in **10**.

of the NR_2 groups. So, if an exchange process can be shown to involve only two of the four signals Me_{cis}^{exo}, Me_{trans}^{exo}, Me_{cis}^{endo}, Me_{trans}^{endo} or only two of the four signals H_{cis}^{exo}, H_{trans}^{exo}, H_{cis}^{endo}, H_{trans}^{endo} then it must necessarily be a correlated Ar–CO and C–N rotation. Similarly, any exchange process which leaves some aromatic protons unchanged (they will be the ones of the naphthyl ring) must be a correlated rotation.

We carried out variable temperature NMR experiments on **10** at 300 MHz in [D_6]DMSO and in $CDCl_3$. Figure 4a shows portions of the NMR spectrum of **10** in [D_6]DMSO at a range of temperatures from 25 to 90 °C; the signals arising from H_{cis} and H_{trans} (four signals) and Me_{cis} and Me_{trans} (four signals) are labelled A-H.

At 25 and 30 °C it is clear that some of the signals (quartets A and C, doublets E and H) are already undergoing exchange, as they are somewhat broadened, and their broadening increases as the temperature rises. An important feature of this spectrum is that only some of the signals are broadened. At 40 °C the situation is even more marked: F and G are still clearly doublets close to the slow exchange limit, while E and H are close to coalescence. At 50 °C, B, D, F and G have also begun to take part in exchange processes, but nonetheless F and G retain doublet structure (and quartet structure is still just visible for B and D) while E and H are fully coalesced. Coalescence of F and G finally occurs at about 60 °C.

There can be no doubt that the process exchanging E and H is faster than the process exchanging F and G since E and H broaden and coalesce sooner than F and G despite being separated by a much greater chemical shift difference (about 70 Hz for E and H; 20 Hz for F and G). This fast process must be a correlated rotation, since it leaves some signals unaffected. Moreover, one diastereoisomer must undergo much faster correlated rotation than the other, because while A and C, and B and D, have similar chemical shift differences, A and C clearly broaden at a lower temperature than B and D.

This simple analysis proves that racemisation of either the *endo* or the *exo* isomer (we have not established which) by correlated rotation is the main rotational process interconverting the conformers of **10**. Using more detailed lineshape analysis[33] we deduced that correlated rotation accounts for more than a third of the rotational processes in **10**; this indicates that it is a simple molecular gear with rate of rotation of the order of 10 Hz at room temperature and a gear-slippage rate of less than one third.

Variable temperature experiments on **10** in $CDCl_3$ (Figure 4b) are less conclusive, and it is possible to draw only general conclusions from the spectra. As the temperature rose above 10 °C, one pair only of Me_{cis}^{exo}, Me_{trans}^{exo}, Me_{cis}^{endo} and

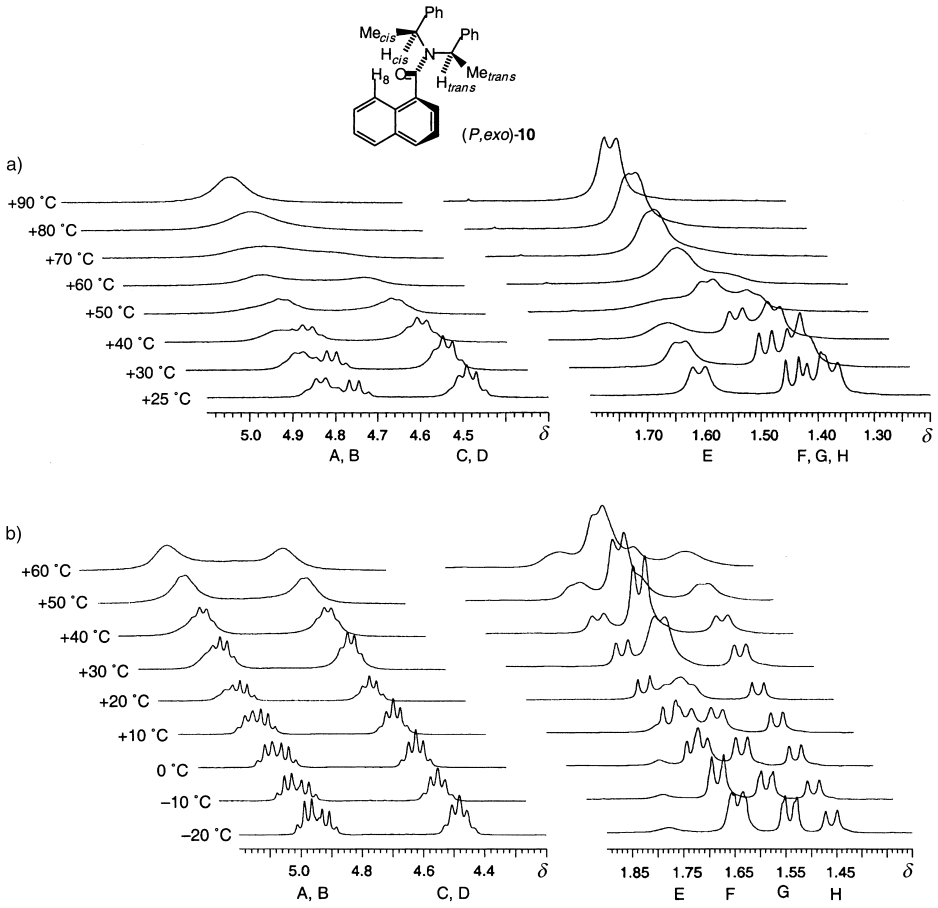

Figure 4. VT NMR of **10** in a) [D_6]DMSO; b) $CDCl_3$.

Me_{trans}^{endo} (signals F and G) broaden, and by 60 °C they coalesce, while the other (E and H) remains sharp to almost 40 °C. However, the significance of the different behaviour of the two sets of peaks is not clear since the broadening pair have a much smaller chemical shift difference than the non-broadening pair. The signals A – D (corresponding to H_{cis}^{exo}, H_{trans}^{exo}, H_{cis}^{endo} and H_{trans}^{endo}) behave similarly. Above 10 °C, signals A and C become broad, up to a temperature of 50 °C, at which the other pair (B and D) also begin to broaden. Given that these two pairs have a very similar chemical shift separation, this difference in behaviour must be due to a concerted rotation.

Variable temperature experiments on **11** were carried out at 300 MHz in CD_3OD and in $[D_6]$DMSO. Coalescence of Me_{trans}^{exo} with Me_{trans}^{endo} and of H_{trans}^{exo} with H_{trans}^{endo} (the *exo* and *endo* conformers had coincident peaks for Me_{cis} and H_{cis}) at about 25 °C in CD_3OD indicated that these peaks interconverted with a barrier of about 59 ± 1 kJ mol^{-1}. Only uncorrelated Ar–CO rotation can account for this interconversion. The coalescence of Me_{cis} with Me_{trans} and of H_{cis} with H_{trans} occurred at about 95 °C in DMSO, and indicated a barrier for C–N rotation (both correlated and uncorrelated) of 73 ± 1 kJ mol^{-1}. For the cyclic **11**, therefore, uncorrelated Ar–CO rotation is the fastest conformational process.

For the chiral (and, incidentally, enantiomerically pure) **12**, there are only *two* conformers, named *exo* and *endo* according to the relationship between the methyl group *trans* to oxygen and the ring. The two conformers are diastereoisomeric and are interconverted by either an Ar–CO or a concerted Ar–CO/C–N rotation. C–N rotation is degenerate, and leaves the molecule unchanged, though it exchanges Me_A and Me_B. Scheme 3 illustrates conformational interconversions in **12**.

Amide **12** lacks some of the advantages afforded **10** by its symmetry, and careful consideration of the signal exchanges associated with each conformational change is required for any information to be gained from VT NMR studies on **12** (which was performed at 300 MHz). C–N rotation will exchange the two methyl doublets of each *exo* diastereoisomer, while Ar–CO rotation will exchange the *cis* methyl group of *exo* with the *cis* methyl group of *endo*. A concerted rotation will exchange the *cis* and *trans* methyl groups of different diastereoisomers. In principle, since signals belonging to the *endo* and *exo* diastereoisomers can be assigned by integration, and signals *cis* or *trans* to O tentatively assigned by chemical shift, clear coalescences between pairs of peaks would indicate the predominant conformational processes in **12**.

Figure 5 shows VT NMR spectra of **12** in $[D_6]$DMSO between 22 and 80 °C; integration of the spectrum at 22 °C allows assignment of the outer pair of methyl doublets to one diastereoisomer (arbitrarily *endo*) and the inner pair to the other (arbitrarily *exo*). Unfortunately, the coalescences shown in Figure 5 are very difficult to analyse—essentially, all four Me groups coalesce to a single signal at about 70 °C. While this

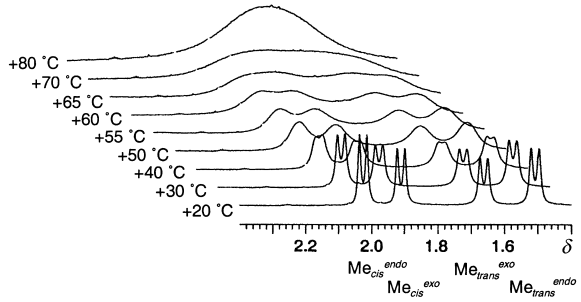

Figure 5. VT NMR of **12** in DMSO.

is consistent with a picture of different mechanisms occurring at similar rates, it neither proves nor disproves correlated rotation.

Saturation transfer experiment on 12: Given the good separation of the methyl doublets in the room temperature spectrum of **12**, we turned to the method of saturation transfer, or more properly inversion transfer, originated by Forsén and Hoffmann,[34] in order to obtain more detailed information on exchanges between the peaks in the spectrum. In a series of four experiments, coupling to the methyl signals was eliminated by irradiating the CHMe quartets, and each methyl signal in turn was selectively inverted and a series of spectra acquired at intervals starting at 0.05 s over the subsequent 5 s period. Figure 6 shows the evolution of the methyl signals following the selective inversion of Me_{cis}^{endo}, and Figure 7 plots the peak height against time for the four peaks. Magnetisation is clearly transferred principally to one other signal—a member of the pair belonging to the other conformer of **12** (Me_{trans}^{exo}).

In order to extract detailed kinetic data from these results, the signal peak heights were normalised to the averaged integrals of peaks assigned to each conformer in the fully relaxed spectra, the ratio of the integrals giving a value for K, the equilibrium constant between the two conformers. The symmetry of **12** is now turned to advantage, since—given K—

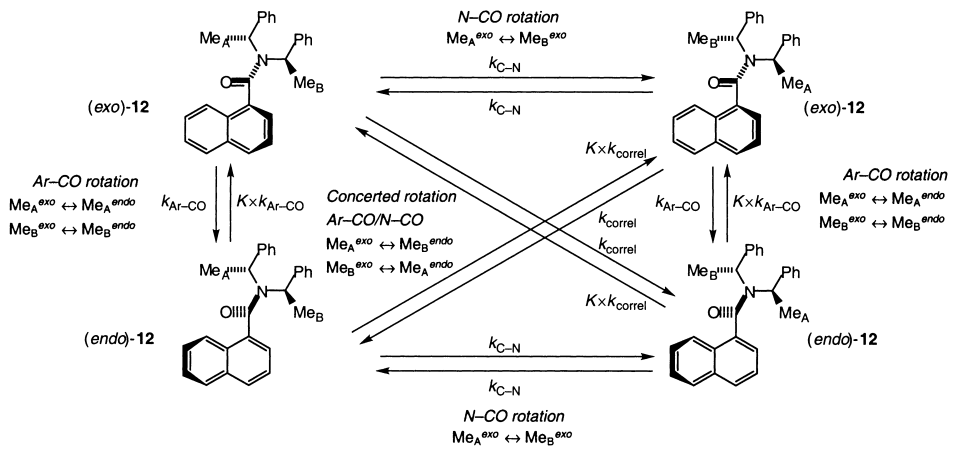

Scheme 3. Conformational changes in C_2-symmetric amide **12**.

0947-6539/02/0806-1284 $ 17.50+.50/0 *Chem. Eur. J.* **2002**, *8*, No. 6

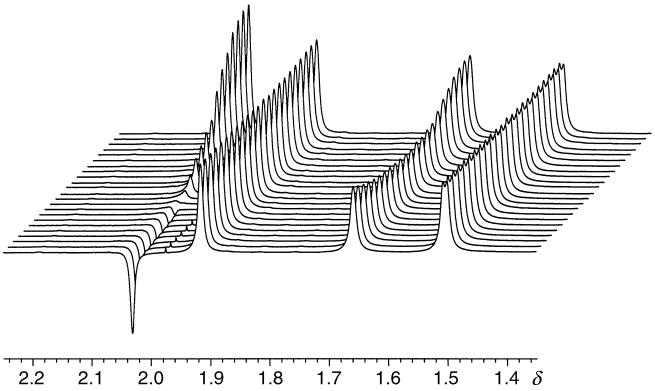

Figure 6. Evolution of the ^{1}H NMR spectrum of **12** in [D_6]DMSO over 5 s following selective inversion of Me_{cis}^{endo}.

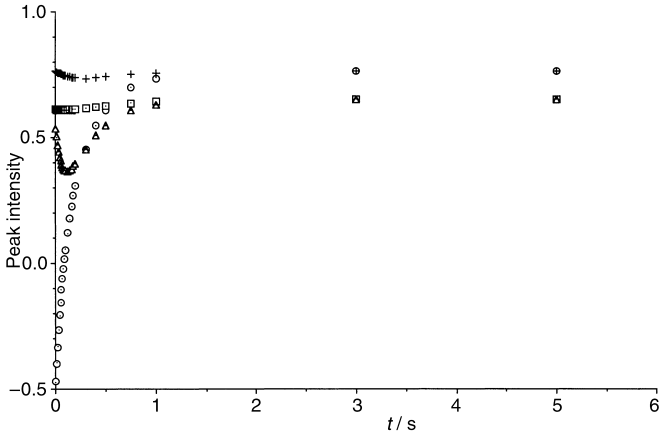

Figure 7. Evolution of the peak intensities in the spectrum of **12** in [D_6]DMSO following selective inversion of Me_{cis}^{endo}. ○ Me_{cis}^{endo}, □ Me_{cis}^{exo}, △ Me_{trans}^{exo}, + Me_{trans}^{endo}.

just three first-order rate constants describe the interconversion of the conformers of **12**, k_{Ar-CO}, k_{C-N} and k_{correl}. These rate constants are represented by rates of interconversion of these four methyl doublets, as shown in Scheme 3. Assignment of the four methyl doublets was made firstly by integration and secondly by assuming that the downfield methyl doublet in each conformer is the one *cis* to oxygen. The results of the saturation transfer experiments were analysed using the program cifit.[35] Initially, cifit was used to fit the normalised experimental peak heights using the mechanism, above, with the four initial and equilibrium peak heights, the T_1 values of all signals, and the three rates as variable parameters. From these fits the T_1 values of the four signals were calculated by averaging the spin lattice relaxation rates estimated for each signal in the two experiments where it was inverted and where it exchanged most rapidly with the inverted signal. The resultant T_1 values were 0.43 s (Me_{cis}^{endo}), 0.44 s (Me_{cis}^{exo}), 0.23 s (Me_{trans}^{exo}) and 0.21 s (Me_{trans}^{endo}), with estimated uncertainties of less than 5%. The T_1 values of all signals were then fixed at these values, and cifit run once again with only the four initial and equilibrium peak heights, and the three rates as variable parameters. The three rate constants were then averaged over the four sets of data, giving values (at 23 °C) of:[36]

$K = 1.695 \pm 0.005$

$k_{Ar-CO} = 0.34 \pm 0.04\ s^{-1}$

$k_{C-N} = -0.0 \pm 0.04\ s^{-1}$

$k_{correl} = 4.27 \pm 0.04\ s^{-1}$

In other words, there is no evidence for C–N rotation occurring without a correlated Ar–CO rotation, and only about 1 in 12 Ar–CO rotations are uncorrelated. Compound **12** is close to being a perfect molecular gear.

EXSY experiment on 3: Previous VT NMR experiments with **3** had led us to speculate that it may undergo conformational change through concerted rotation.[4] Unlike **12**, however, assignment of peaks in **3** is not straightforward because the two conformers of **3** are enantiomeric and not diastereoisomeric. Furthermore, the pairs of doublets, even in DMSO where they are best separated, lie rather too close for selective perturbation. The solution was to use EXSY both to assign the diastereotopic methyl groups of **3** and to follow the transfer of saturation between the signals. We were helped by the fact that *N*,*N*-diisopropylnaphthamides appear to adopt a well-defined conformation in solution (illustrated by the X-ray crystal structure of **3**[37] and shown in Figure 8) in which the

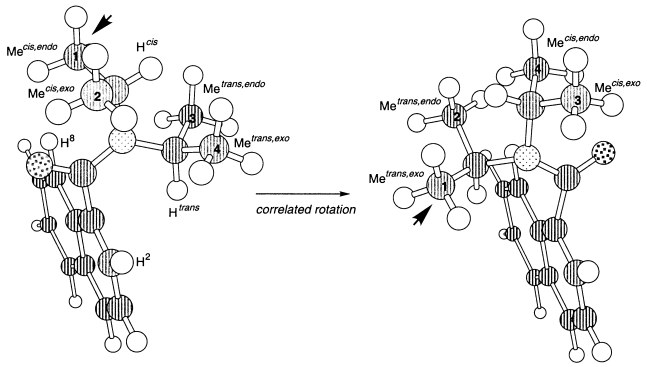

Figure 8. Conformation of **3** and the choreography of a correlated rotation.

isopropyl group *cis* to oxygen straddles the C=O group while the isopropyl group *trans* to oxygen in turn straddles the Me_2C–H bond of the other isopropyl group. A preliminary COSY experiment facilitated assignment of protons in the aromatic region.

Details of the 400 MHz EXSY spectrum of 3, acquired with a mixing time of 300 ms, are shown in Figure 9. Cross-peaks between the two *trans* methyl groups and H^{cis} (Figure 9b) are much stronger than cross-peaks between the two *cis* methyl groups and H^{trans}, adding further evidence that Figure 8 represents the preferred conformation of **3** in solution. The cross-peaks in the aromatic region (Figure 9a) confirmed the COSY assignment and allowed a definitive assignment of the 2- and 8-protons of the naphthalene ring, as shown. This consequently allowed us to assign each of the diastereotopic methyl doublets either *exo* or *endo* stereochemistry: The two

exo protons have clear cross-peaks with H^2, while the two *endo* protons have cross-peaks with H^8. This leads to the assignment of the four methyl doublets as $Me^{cis,endo}$, $Me^{cis,exo}$, $Me^{trans,exo}$, $Me^{trans,endo}$ (respectively from low to high field), as shown in Figure 8.

The EXSY experiment also gives detailed information on the transfer of saturation from one methyl doublet to another, and the cross-peaks between the methyl doublets clearly indicate that the major process taking place is the one which interconverts $Me^{cis,endo}$ with $Me^{trans,exo}$—a correlated rotation (see Figure 8). Smaller cross-peaks are visible for the interconversion of the *endo* and *exo* methyl groups within each isopropyl group, corresponding to Ar–CO rotation. The lack of a cross-peak between the two *exo* or two *endo* peaks indicates that C–N rotation, as for **12**, is very slow.

Integration of the EXSY diagonal cross-peak volumes using the standard Vnmr software allowed us to estimate rate constants for k_{Ar-CO}, k_{C-N} and k_{corel} as shown below: Again, correlated rotation is by far the most important process in **3**, accounting for essentially all C–N rotation and over 90% of Ar–CO rotation:

$k_{Ar-CO} \approx 0.04\ s^{-1}$

$k_{C-N} \approx 0\ s^{-1}$

$k_{correl} \approx 0.64\ s^{-1}$

Correlated rotation in a 2-substituted naphthamide: Having proved correlated rotation in two naphthamides bearing branched N-substituents, we were keen to know whether correlated rotation also occurs in more hindered systems such as 2-substituted 1-naphthamides. Such compounds are atropisomeric, and we have determined their rates of Ar–CO rotation to be typically of the order of $10^{-5}\ s^{-1}$ at 20 °C (half-lives of the order of hours, days or weeks) by following their racemisation after chromatographic resolution. Rotations occurring with rates of less than about $0.01\ s^{-1}$ are not amenable to study by NMR methods, so we decided to use a similar separation/isomerisation method for our study.

In order to distinguish the various types of rotation possi-

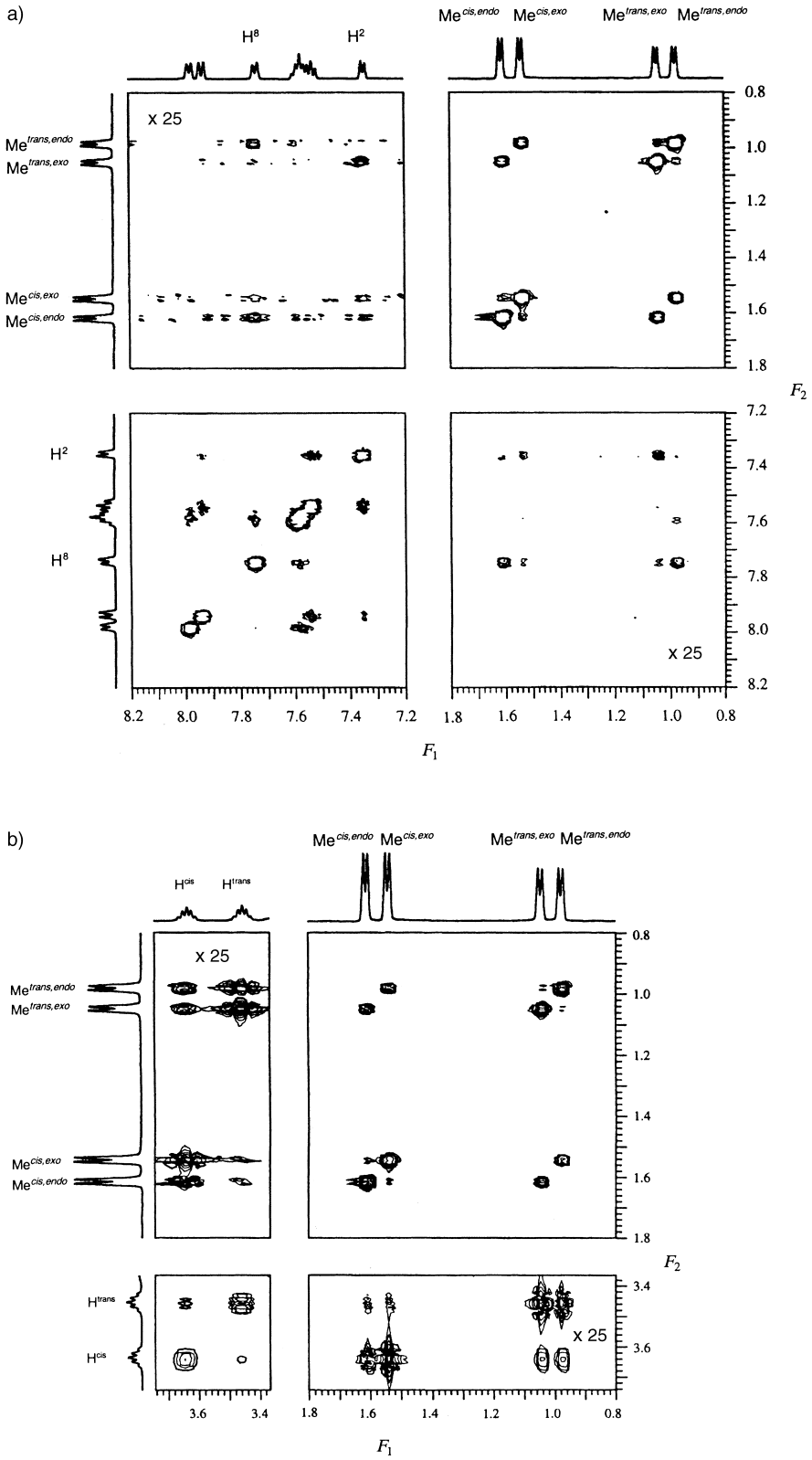

Figure 9. EXSY spectrum of **3** in [D_6]DMSO at 22 °C. a) $H^{2,8}$ and Me cross-peaks; b) $H^{cis,trans}$ and Me cross-peaks.

0947-6539/02/0806-1286 $ 17.50+.50/0 *Chem. Eur. J.* **2002**, *8*, No. 6

ble, we require a compound with four possible conformers, and to simplify both assignment and analysis we chose **13**, which has the same symmetry as **10** and **11**, in that its conformers comprise the two enantiomers of each of two diastereoisomers. As with **10**, its symmetry means that there are four possible conformational processes, as shown in Scheme 4 (K is the equilibrium constant for interconversion of the diastereoisomers).

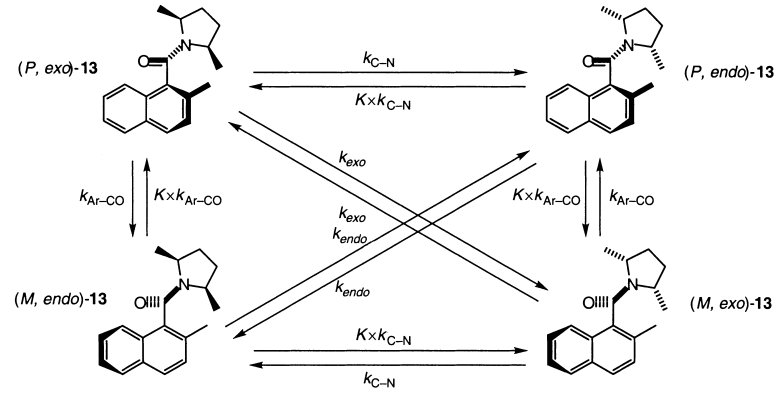

Scheme 4. Conformational changes in amide **13**.

Non-correlated Ar–CO and C–N rotations interconvert diastereoisomers, with each leading to a different enantiomer. Assignment of stereochemistry for all four conformers of **13** will be necessary to distinguish these two rotations. However, the correlated rotation we are seeking to prove interconverts enantiomers, and enantiomers are immediately recognisable by their 1:1 ratio in an HPLC trace. A very important point about the design of **13** is therefore that *no assignment of stereochemistry to the conformers of **13** is required* for identification of correlated rotation: it is the only process interconverting conformers present in a 1:1 ratio in a racemic mixture of **13**.

Compound **13** was made straightforwardly by ortholithiation of **11**, and was resolvable into its four atropisomeric stereoisomers by flash chromatography followed by preparative HPLC on Chiralpak-AD stationary phase. Ratios of isomers in mixtures were determined by a combination of HPLC on chiral and achiral stationary phases. Although it not essential to the conclusions we shall draw from this study, the analysis is clarified by a tentative assignment of stereochemistry to the atropisomers of **13**. Relative stereochemistry (*exo* and *endo*) was assigned by NOE experiments; absolute stereochemistry was assigned by comparing the retention times of the two pairs of enantiomers on a Whelk-O1 chiral column and by use of Pirkle's model[10] for binding to this chiral stationary phase.

We then took samples of (*P*, *exo*)-**13** and (*P*, *endo*)-**13** and allowed them to equilibrate with their stereoisomers by incubating them separately in hexane at 33 °C and analysed the resulting product mixture at intervals. The results for (*P*, *endo*)-**13** are shown in Figure 10. Kinetic analysis is simplified by the fact that enantiomeric processes must have the same activation energy, and also by the fact that K, the ratio of (±, *exo*)- to (±, *endo*)-**3** at equilibrium, could be determined accurately (1.28 ± 0.02) by HPLC and confirmed by NMR. Four mechanistic rate constants are involved: $k_{Ar–CO}$, for rotation about the Ar–CO bond *exo* to *endo*, $k_{C–N}$, for rotation of the *exo* isomer about the C–N bond *exo* to *endo*, and k_{exo} and k_{endo} for the proposed concerted enantiomerisations of the two diastereoisomers. Rates for the reverse Ar–CO and C–N rotations (*endo* to *exo*) are then related to $k_{Ar–CO}$ and $k_{C–N}$ by the equilibrium constant K.

It is immediately clear from the plot that the rate at which (*P*, *endo*)-**13** enantiomerises to (*M*, *endo*)-**13** is greater than the rate at which it undergoes rotation about the Ar–CO bond, and so rotation about the Ar–CO bond must be concerted to some degree with rotation about the C–N bond. In order to extract rate constants from this data, the mechanism shown in Scheme 4 was simplified by assuming $k_{Ar–CO} = 0$. A least-squares fit using the data ob-

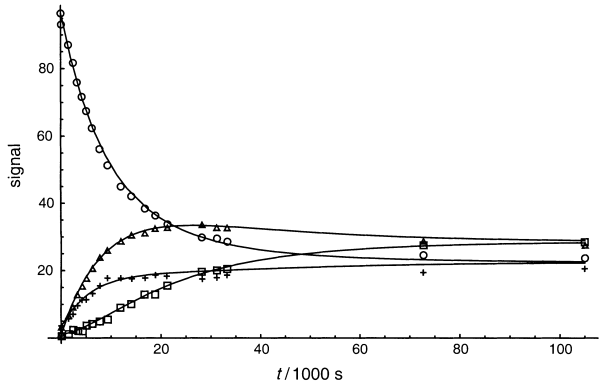

Figure 10. Evolution of the composition of a sample of (*P*, *endo*)-**13** with time in hexane at 33 °C. ○ (*P*, *endo*)-**13**, △ (*P*, *exo*)-**13**, + (*M*, *endo*)-**13**, □ (*M*, *exo*)-**13**. Solid lines indicate evolution calculated by iterative fitting.

tained from both (*P*, *exo*)-**13** and (*P*, *endo*)-**13** then gave values for $k_{C–N}$, k_{exo} and k_{endo} at 33 °C for the four processes:

$K = 1.30 \pm 0.05$

$k_{Ar–CO} = 0\ s^{-1}$

$k_{C–N} = 4.0 \pm 0.3 \times 10^{-5}\ s^{-1}$

$k_{exo} = 1.2 \pm 0.3 \times 10^{-5}\ s^{-1}$

$k_{endo} = 3.0 \pm 0.2 \times 10^{-5}\ s^{-1}$

It is important to note that irrespective of the tentative assignments of stereochemistry, k_{exo} and k_{endo} represent correlated rotations. The fact that k_{exo} and k_{endo} are not zero confirms that concerted rotation takes place, and since k_{exo} and k_{endo} must be at least an order of magnitude larger than

k_{Ar-CO}, at least 90% of rotations about the Ar–CO bond are concerted with a rotation about the C–N bond. As k_{C-N} has the same magnitude as $k_{exo}+k_{endo}$, C–N rotations must also be free to occur in a non-concerted manner, and occur about as frequently as concerted C–N/Ar–CO rotations.

Conclusion

Gearing effects in amide rotations: Table 3 summarises the rate constants for rotation of the four amides **3**, **10**, **12** and **13**, along with barriers $\Delta G^{\ddagger}$ for each process calculated using the Eyring equation. Previous results[4] had shown that aromatic amides with unbranched N-substituents undergo Ar–CO rotation significantly faster than C–N rotation: Ar–CO rotation must be able to occur without concurrent C–N rotation, though it is possible that C–N rotations are still correlated with Ar–CO rotations. With branched N-substituents, uncorrelated Ar–CO rotation is much slower, and the results presented in this paper indicate that it occurs almost solely in correlation with C–N rotation, which remains. Uncorrelated C–N rotation appears to be even rarer, and essentially never occurs in 2-unsubstituted naphthamides with branched N-substituents. Increasing steric hindrance still further by introducing a substituent at the 2-position of the ring essentially shuts down uncorrelated Ar–CO rotation—almost all Ar–CO rotation is correlated. Uncorrelated C–N can now take place, and only about 50% is correlated with Ar–CO rotation.

Table 3. Summary of rates of rotation.

	3 at 22 °C[a]	**10** at 23 °C[29][a]	**12** at 22 °C[a]	**13** at 33 °C[b]
uncorrelated	$k_{Ar-CO} = 0.04\ s^{-1}$		$k_{Ar-CO} = 0.34\ s^{-1}$	$k_{Ar-CO} < 0.1 \times 10^{-5}\ s^{-1}$
	$\Delta G^{\ddagger} = 80.1\ kJ\,mol^{-1}$	$k = 2.5\ s^{-1}$	$\Delta G^{\ddagger} = 74.9\ kJ\,mol^{-1}$	$\Delta G^{\ddagger} > 110\ kJ\,mol^{-1}$
	$k_{C-N} = 0$	$\Delta G^{\ddagger} = 70.2\ kJ\,mol^{-1}$	$k_{C-N} = 0$	$k_{C-N} = 4.0 \times 10^{-5}\ s^{-1}$
				$\Delta G^{\ddagger} = 100.8\ kJ\,mol^{-1}$
correlated				$k_{exo} = 1.2 \times 10^{-5}\ s^{-1}$
	$k = 0.64\ s^{-1}$	$k = 6.7\ s^{-1}$	$k = 4.27\ s^{-1}$	$\Delta G^{\ddagger} = 103.9\ kJ\,mol^{-1}$
	$\Delta G^{\ddagger} = 73.3\ kJ\,mol^{-1}$	$\Delta G^{\ddagger} = 67.8\ kJ\,mol^{-1}$	$\Delta G^{\ddagger} = 68.7\ kJ\,mol^{-1}$	$k_{endo} = 3.0 \times 10^{-5}\ s^{-1}$
				$\Delta G^{\ddagger} = 101.6\ kJ\,mol^{-1}$

[a] In [D_6]DMSO. [b] In hexane.

Experimental Section

Compounds **4**–**9**, **11** and **12** were made by acylation of the corresponding known or available amines by the following general procedure. 1-Naphthoyl chloride or benzoyl chloride (1.5 mmol) was added dropwise to a solution of the amine (1.0 mmol), triethylamine (3.0 mmol) and dichloromethane (10 mL) at 0 °C. Stirring was continued at room temperature for 16 h. The reaction mixture was then diluted with dichloromethane (10 mL) and washed with 1M hydrochloric acid (20 mL × 2), water (20 mL × 2), brine (20 mL), dried ($MgSO_4$), and the solvent removed under reduced pressure to yield a crude product which was purified by crystallisation or chromatography. Compounds **10** and **13** were made by lithiation and methylation of **4** and **11**.

***N*-Benzyl-*N*-[(1*S*)-1-phenylethyl]-1-naphthamide (4)**: The crude product was recrystallised from ethyl acetate to give the naphthamide **4** (6.65 g, 39%) as prisms. M.p. 100–102 °C (from EtOAc); R_f (petroleum ether/EtOAc 2:1) = 0.48; $[\alpha] = -139.6$ ($c = 3.8$ in EtOH); IR (film): $\nu_{max} = 1632\ cm^{-1}$ (C=O); ^1H (300 MHz, $CDCl_3$, −20 °C): $\delta = 8.2-6.9$ (m, 17 $H^{maj,min}$, ArH), 6.47 (q, 1 $H^{min'}$, $J = 7$ Hz, C*H*Me), 6.27 (q, 1 $H^{min''}$, $J = 7$ Hz, C*H*Me), 5.83 (d, 1 $H^{maj''}$, $J = 15$ Hz, CH_AH_B), 5.19 (d, 1 $H^{maj'}$, $J = 15.5$ Hz, CH_AH_B), 4.98 (q, 1 $H^{maj'}$, $J = 7$ Hz, C*H*Me), 4.96 (q, 1 $H^{maj''}$, $J = 7$ Hz, C*H*Me), 4.41 (d, 1 $H^{min''}$, $J = 16$ Hz, CH_AH_B), 4.19 (d, 1 $H^{min'}$, $J = 16.5$ Hz, CH_AH_B), 4.10 (d, 1 $H^{maj''}$, $J = 15$ Hz, CH_AH_B), 4.04 (d, 1 $H^{min'}$, $J = 16$ Hz, CH_AH_B), 4.03 (d, 1 $H^{maj'}$, $J = 15.5$ Hz, CH_AH_B), 3.98 (d, 1 $H^{min'}$, $J = 16.5$ Hz, CH_AH_B), 1.72 (d, 3 H'', $J = 7$ Hz, Me), 1.52 (d, 3 $H^{min'}$, $J = 7$ Hz, Me), 1.44 (d, 3 $H^{maj'}$, $J = 7$ Hz, Me), 1.33 (d, 3 $H^{maj''}$, $J = 7$ Hz, Me); MS: *m/z*: calcd for $C_{26}H_{23}NO$: 365.1780; found: 365.1773 $[M]^+$; CI-MS: *m/z* (%): 366 (100) $[MH]^+$; elemental analysis calcd (%) for $C_{26}H_{23}NO$: C 85.3, H 6.3, N 3.9; found: C 85.5, H 6.3, N 3.8.

***N*-Benzyl-*N*-[(1*S*)-1-(1-naphthyl)ethyl]-1-naphthamide (5)**: The crude product which was purified by flash column chromatography, eluting with petroleum ether/EtOAc 10:1, to give the naphthamide **5** (496 mg, 84%) as a foam. R_f (petroleum ether/EtOAc 10:1) = 0.07; $[\alpha] = +151.9$ ($c = 1.1$ in EtOH); IR (film): $\nu_{max} = 1625\ cm^{-1}$ (C=O); ^1H (300 MHz; $CDCl_3$, −20 °C): $\delta = 8.6-6.4$ (m, 19 $H^{maj,min}$, ArH), 7.01 (q, 1 $H^{maj''}$, $J = 7$ Hz, C*H*Me), 6.90 (q, 1 $H^{maj'}$, $J = 7$ Hz, C*H*Me), 5.78 (q, 1 $H^{min'}$, $J = 7$ Hz, C*H*Me), 5.58 (d, 1 $H^{min''}$, $J = 15$ Hz, CH_AH_B), 5.52 (q, 1 $H^{min''}$, $J = 7$ Hz, C*H*Me), 4.90 (d, 1 $H^{min'}$, $J = 15$ Hz, CH_AH_B), 4.55 (d, 1 $H^{min''}$, $J = 15$ Hz, CH_AH_B), 4.36 (d, 1 $H^{min'}$, $J = 15$ Hz, CH_AH_B), 4.31 (d, 1 $H^{maj''}$, $J = 16$ Hz, CH_AH_B), 4.13 (d, 1 $H^{maj'}$, $J = 16$ Hz, CH_AH_B), 3.66 (d, 1 $H^{maj''}$, $J = 16$ Hz, CH_AH_B), 3.53 (d, 1 $H^{maj'}$, $J = 16$ Hz, CH_AH_B), 1.77 (d, 3 $H^{maj''}$, $J = 7$ Hz, Me), 1.64 (d, 3 $H^{maj'}$, $J = 7$ Hz, Me), 1.56 (d, 3 $H^{min''}$, $J = 7$ Hz, Me), 1.44 (d, 3 $H^{min'}$, $J = 7$ Hz, Me); MS: *m/z*: calcd for $C_{30}H_{26}NO$: 416.2014; found: 416.2032 $[MH]^+$; CI-MS: *m/z* (%): 416 (100) $[MH]^+$.

***N*-(1-Methylethyl)-*N*-[(1*S*)-1-phenylethyl]-1-naphthalenecarboxamide (6)**: The crude product was purified by flash column chromatography, eluting with petroleum ether/EtOAc 5:1, to yield the naphthamide **6** (583 mg, 85%) as a foam. R_f (petroleum ether/EtOAc 5:1) = 0.13; $[\alpha] = -148.6$ ($c = 2.7$ in EtOH); IR (film): ν_{max}: 1631 cm^{-1} (C=O); ^1H (300 MHz; $CDCl_3$, −20 °C): $\delta = 8.2-7.1$ (m, 12 $H^{maj,min}$, ArH), 4.9–4.6 (m, 1 $H^{maj,min}$, C*H*Me), 3.86 (sept, 1 $H^{min'}$, $J = 7$ Hz, C*H*Me_2), 3.81 (sept, 1 $H^{min''}$, $J = 7$ Hz, C*H*Me_2), 3.36 (sept, 1 $H^{maj''}$, $J = 7$ Hz, C*H*Me_2), 3.34 (sept, 1 $H^{maj'}$, $J = 7$ Hz, C*H*Me_2), 2.13 (d, 6 $H^{min'}$, $J = 7$ Hz, 2 × Me), 2.03 (d, 3 $H^{min''}$, $J = 7$ Hz, Me), 1.74 (d, 3 $H^{maj'}$, $J = 7$ Hz, $CHMe_AMe_B$), 1.65 (d, 3 $H^{maj''}$, $J = 7$ Hz, $CHMe_AMe_B$), 1.59 (d, 3 $H^{maj''}$, $J = 7$ Hz, C*H*Me), 1.44 (d, 3 $H^{maj'}$, $J = 7$ Hz, C*H*Me), 1.31 (d, 3 H^{maj}, $J = 7$ Hz, $CHMe_AMe_B$), 1.23 (d, 3 $H^{maj''}$, $J = 7$ Hz, $CHMe_AMe_B$), 1.17 (d, 6 $H^{min''}$, $J = 7$ Hz, 2 × Me), 1.12 (d, 3 $H^{min'}$, $J = 7$ Hz, Me); MS: *m/z*: calcd for $C_{22}H_{23}NO$: 317.1780; found: 317.1783 $[M]^+$; CI-MS: *m/z* (%): 318 (100) $[MH]^+$; elemental analysis calcd (%) for $C_{22}H_{23}NO$: C 83.2, H 7.4, N 4.3; found: C 83.2, H 7.3, N 4.4.

***N*-Benzyl-*N*-[(1*S*)-1-phenylethyl]benzamide (8)**: The crude product was purified by flash column chromatography, eluting with petroleum ether/EtOAc 6:1, to yield the benzamide **8**, (721 mg, 81%) as prisms. M.p. 69–70 °C (from EtOAc); R_f (petroleum ether/EtOAc 5:1) = 0.20; $[\alpha] = -127.8$ ($c = 1.9$ in EtOH); IR (film): $\nu_{max} = 1637\ cm^{-1}$ (C=O); ^1H (300 MHz; $CDCl_3$, −20 °C): $\delta = 7.7-6.9$ (m, 15 $H^{maj,min}$, ArH), 6.12 (q, 1 H^{min}, $J = 7$ Hz, C*H*Me), 5.24 (q, 1 H^{maj}, $J = 7$ Hz, C*H*Me), 5.09 (d, 1 H^{maj}, $J = 15.5$ Hz, CH_AH_B), 4.49 (d, 1 H^{min}, $J = 17$ Hz, CH_AH_B), 4.05 (d, 1 H^{min}, $J = 17$ Hz, CH_AH_B), 3.85 (d, 1 H^{maj}, $J = 15.5$ Hz, CH_AH_B), 1.48 (d, 3 $H^{maj,min}$, $J = 7$ Hz, Me); MS: *m/z*: calcd for $C_{22}H_{21}NO$: 316.1701; found: 316.1708 $[MH]^+$; CI-MS: *m/z* (%): 316 (100) $[MH]^+$; elemental analysis calcd (%) for $C_{22}H_{21}NO$: C 83.7, H 6.9, N 4.5; found: C 83.8, H 6.7, N 4.4.

1-[*N*-(2,5-*cis*-Dimethyl)pyrrolidinylcarbonyl]naphthalene (11): The crude product was purified by recrystallisation from EtOAc to yield the naphthamide **11** (2.89 g, 78%). M.p. 118–119 °C; IR (film): $\nu_{max} = 1618\ cm^{-1}$; ^1H (300 MHz; $CDCl_3$): $\delta = 7.92-7.78$ (m, 3H, ArH), 7.60–7.42 (m, 4H, ArH), 4.52 (sextet, 1H, $J = 6.5$ Hz, *exo*-NCH), 3.65 (br s, 1H, *endo*-NCH), 2.33–1.48 (m, 4H, 2 × CH_2), 1.59 (d, 3H, $J = 6.5$ Hz, *exo*-NCHCH_3), 0.90 (br s, 3H, *endo*-NCHCH_3); ^{13}C (75 MHz; $CDCl_3$): $\delta = 169.2$ (s, CO),

0947-6539/02/0806-1288 $ 17.50+.50/0 *Chem. Eur. J.* **2002**, *8*, No. 6

135.9 (s, Ar), 133.4 (d, Ar), 128.6 (d, Ar), 128.2 (d, Ar), 126.8 (d, Ar), 126.2 (d, Ar), 126.1 (d, Ar), 125.0 (d, Ar), 123.2 (s, Ar), 55.6 (d, NCH), 53.8 (d, NCH), 32.1 (t, CH_2), 31.2 (t, CH_2), 22.2 (q, CH_3), 22.0 (q, CH_3); MS: *m*/*z*: calcd for $C_{17}H_{19}NO$: 253.1467; found: 253.1465; CI-MS: *m*/*z* (%): calcd for 253.1467 $[M]^+$; found: 254 (100), 155 (8); elemental analysis calcd (%) for $C_{17}H_{19}NO$: C 80.60, H 7.56, N 5.53; found: C 80.35, H 7.56, N 5.43.

1-[*N*-(2,5-*cis*-Dimethyl)pyrrolidinylcarbonyl]-2-methylnaphthalene (13): *s*-Butyllithium (0.167 mL, 1.3 M solution in cyclohexane, 0.217 mmol) was added dropwise to a solution of **11** (50 mg, 0.197 mmol) in THF (20 mL), cooled to −78 °C under an atmosphere of nitrogen. The resulting yellow solution was then stirred for 50 min before the addition of methyl iodide (18 μL, 0.295 mmol). After a further 1 h at −78 °C the solution was warmed to room temperature. Once the reaction mixture had turned colourless, water (20 mL) was added and the THF was removed under reduced pressure. The aqueous phase was extracted with dichloromethane (3 × 20 mL) and the combined extracts washed with water (20 mL) and dried over magnesium sulfate. The solution was filtered and the solvent was evaporated. Purification by column chromatography (light petroleum/ethyl acetate 7:3) afforded the two diastereoisomers of 1-[*N*-(2,5-dimethyl)pyrrolidinylcarbonyl]-2-methylnaphthalene (49 mg, 93%) as white solids. Fraction 1 was assigned *exo* stereochemistry: IR (nujol): $\nu_{max} = 1619\ cm^{-1}$; ^1H (300 MHz; $CDCl_3$): $\delta = 7.89$ (m, 1H, ArH), 7.79 (d, 1H, $J = 8.5$ Hz, ArH), 7.63–7.42 (m, 3H, ArH), 7.37 (d, 1H, $J = 8.5$ Hz, ArH), 4.58 (sextet, 1H, $J = 7$ Hz, NCH), 3.52 (double quintet (dqn), 1H, $J = 6.5$, 2 Hz, NCH), 2.54 (s, 3H, $ArCH_3$), 2.34–2.20 (m, 1H, CH_2), 2.00–1.73 (m, 2H, CH_2), 1.64–1.52 (m, 1H, CH_2), 1.60 (d, 3H, $J = 6$ Hz, $NCHCH_3$), 0.91 (d, 3H, $J = 7$ Hz, $NCHCH_3$); ^{13}C (75 MHz; $CDCl_3$): $\delta = 168.9$ (s, CO), 134.2 (s, Ar), 132.0 (s, Ar), 131.6 (s, Ar), 129.2 (s, Ar), 128.5 (d, Ar), 128.2 (d, Ar), 128.1 (d, Ar), 126.9 (d, Ar), 125.2 (d, Ar), 123.8 (d, Ar), 55.4 (d, NCH), 53.6 (d, NCH), 32.3 (t, CH_2), 31.2 (t, CH_2), 22.0 (q, $NCHCH_3$), 21.4 (q, $NCHCH_3$), 19.6 (q, $ArCH_3$); CI-MS: *m*/*z* (%): calcd for $C_{18}H_{21}NO$: 267.1623; found: 267.1617 $[M]^+$, 268 (100), 169 (8). The enantiomers were separated by HPLC on a Chiralpak AD 250 × 10 mm column, eluent 10% EtOH in hexane, flow 2.4 mL min^{-1}, UV at 280 nm, $t_R = 11.46$ and 19.42 min.

Fraction 2 was assigned *endo* stereochemistry: IR (nujol): $\nu_{max} = 1623\ cm^{-1}$; ^1H (300 MHz; $CDCl_3$): $\delta = 7.74–7.64$ (m, 2H, ArH), 7.46–7.32 (m, 2H, ArH), 7.23 (d, 1H, $J = 8.5$ Hz), 4.41 (sextet, 1H, $J = 7$ Hz, NCH), 3.52 (qnd, 1H, $J = 6$, 2 Hz, NCH), 2.32 (s, 3H, $ArCH_3$), 2.23–2.09 (m, 1H, CH_2), 1.94–1.65 (m, 2H, CH_2), 1.55 (d, 3H, $J = 6$ Hz, $CHMe$), 1.53–1.44 (m, 1H, CH_2), 0.61 (d, 3H, $J = 8.5$ Hz, $CHMe$); ^{13}C (75 MHz; $CDCl_3$): $\delta = 168.9$ (s, CO), 134.4 (s, Ar), 131.8 (s, Ar), 130.3 (s, Ar), 130.0 (s, Ar), 128.2 (d, Ar), 128.1 (d, Ar), 127.8 (d, Ar), 126.5 (d, Ar), 125.3 (d, Ar), 125.1 (d, Ar), 55.6 (d, NCH), 53.6 (d, NCH), 32.5 (t, CH_2), 31.3 (t, CH_2), 22.1 (q, CH_3), 21.8 (q, CH_3), 19.2 (q, $ArCH_3$); CI-MS: *m*/*z* (%): calcd for $C_{18}H_{21}NO$: 267.1623; found: 268 (100), 267.1625 $[M]^+$, 254 (13), 169 (5). The enantiomers were separated by HPLC on a Chiralpak AD 250 × 10 mm column, Merck-Hitachi system, eluent 10% EtOH in hexane, flow 2.4 mL min^{-1}, UV at 280 nm, $t_R = 11.33$ and 13.13 min.

The *exo* and *endo* diastereoisomers were separable on a Phenosphere HPLC column (100 × 8 mm), eluent 5% ethanol in hexane, flow 2 mL min^{-1}, $t_R =$ 5.34 (*exo*) and 6.42 min (*endo*).

Mixtures of stereoisomers of **13** were analysed by HPLC on a Chiralpak AD 250 × 10 mm to determine the ratio of [(*M*, *exo*) + (*M*, *endo*)]-[(*P*, *endo*) + (*P*, *exo*)] (both diastereoisomers of *M*-**13** co-elute from this column) followed by HPLC on a silica Phenosphere column (100 × 8.00 mm) to determine the ratio of [(*M*, *exo*) + (*P*, *exo*)]:[(*M*, *endo*) + (*P*, *endo*)].

Acknowledgement

We are grateful for studentships from the EPSRC (to R.A.B.) and for funding from the Leverhulme Trust, Oxford Asymmetry and the Royal Society. We thank Dr. Madeleine Helliwell for carrying out the X-ray crystal structure determination of **4** and **7**, and Lai Wah Lai and Ghokulan Tharmaratnam for making **7** and **11**. Dr. Alex Bain kindly provided the program cifit.

[1] P. Bowles, J. Clayden, M. Helliwell, C. McCarthy, M. Tomkinson, N. Westlund, *J. Chem. Soc. Perkin Trans. 1* **1997**, 2607.
[2] J. Clayden, *Angew. Chem.* **1997**, *109*, 986; *Angew. Chem. Int. Ed.* **1997**, *36*, 949.
[3] J. Clayden, in *Organic Synthesis Highlights IV* (Ed.: H.-G. Schmalz), Wiley-VCH, Weinheim, **2000**, pp. 48–52.
[4] A. Ahmed, R. A. Bragg, J. Clayden, L. W. Lai, C. McCarthy, J. H. Pink, N. Westlund, S. A. Yasin, *Tetrahedron* **1998**, *54*, 13277.
[5] J. Clayden, C. McCarthy, M. Helliwell, *Chem. Commun.* **1999**, 2059.
[6] P. Beak, A. Tse, J. Hawkins, C. W. Chen, S. Mills, *Tetrahedron* **1983**, *39*, 1983.
[7] P. M. van Lier, G. H. W. M. Meulendijks, H. M. Buck, *Recl. Trav. Chim. Pays-Bas* **1983**, *102*, 337.
[8] J. Hauer, E. Treml, H. D. Lüdemann, *J. Chem. Res.* (*M*) **1982**, 501.
[9] M. A. Cuyegkeng, A. Mannschreck, *Chem. Ber.* **1987**, *120*, 803.
[10] W. H. Pirkle, C. J. Welch, A. J. Zych, *J. Chromatography* **1993**, *648*, 101.
[11] F. Gasparrini, D. Misiti, M. Pierini, C. Villani, *Tetrahedron*: *Asymmetry* **1997**, *8*, 2069.
[12] M. Oki, *Top. Stereochem.* **1983**, *14*, 1.
[13] J. Clayden, *Synlett* **1998**, 810.
[14] J. Clayden, J. H. Pink, *Tetrahedron Lett.* **1997**, *38*, 2565.
[15] J. Clayden, J. H. Pink, S. A. Yasin, *Tetrahedron Lett.* **1998**, *39*, 105.
[16] J. Clayden, N. Westlund, F. X. Wilson, *Tetrahedron Lett.* **1999**, *40*, 3331.
[17] J. Clayden, L. W. Lai, *Angew. Chem.* **1999**, *111*, 2755; *Angew. Chem. Int. Ed.* **1999**, *38*, 2556.
[18] J. Clayden, P. Johnson, J. H. Pink, M. Helliwell, *J. Org. Chem.* **2000**, *65*, 7033.
[19] J. Clayden, L. W. Lai, *Tetrahedron Lett.* **2001**, *42*, 3163.
[20] J. Clayden, L. W. Lai, M. Helliwell, *Tetrahedron*: *Asymmetry* **2001**, *12*, 695.
[21] J. Sandström, *Dynamic NMR Spectroscopy*, Academic Press, London, **1982**.
[22] D. Kost, E. H. Carlson, M. Raban, *Chem. Commun.* **1971**, 656.
[23] D. Kost, A. Zeichner, *Tetrahedron Lett.* **1974**, 4533.
[24] W. H. Stewart, T. H. Siddall, *Chem. Rev.* **1970**, *70*, 517.
[25] L. Lefrançois, M. Hébraut, C. Tondre, J.-J. Delpuech, C. Berthon, C. Madic, *J. Chem. Soc. Perkin Trans. 2* **1999**, 1149.
[26] U. Berg, J. Sandström, W. B. Jennings, D. Randall, *J. Chem. Soc. Perkin Trans. 2* **1980**, 949.
[27] M. Kuttenberger, M. Frieser, M. Hofweber, A. Mannschreck, *Tetrahedron*: *Asymmetry* **1998**, *9*, 3629.
[28] Preliminary communication 1: J. Clayden, J. H. Pink, *Angew. Chem.* **1998**, *110*, 2040; *Angew. Chem. Int. Ed.* **1998**, *37*, 1937.
[29] Preliminary communication 2: R. A. Bragg, J. Clayden, *Org. Lett.* **2000**, *2*, 3351.
[30] A. H. Lewin, M. Frucht, K. V. J. Chen, E. Benedetti, B. di Blasio, *Tetrahedron* **1975**, *31*, 207.
[31] A. H. Lewin, M. Frucht, *Org. Magn. Reson.* **1975**, *7*, 206.
[32] CCDC-170629 (**4**) and -170630 (**7**) contain the supplementary crystallographic data for this paper. These data can be obtained free of charge via www.ccdc.cam.ac.uk/conts/retrieving.html (or from the Cambridge Crystallographic Data Centre, 12 Union Road, Cambridge CB2 1EZ, UK; (fax: (+44) 1223-336-033; or e-mail: deposit@ccdc.cam.ac.uk).
[33] Details of the method are described in ref. [29].
[34] S. Forsén, R. A. Hoffmann, *J. Chem. Phys.* **1963**, *39*, 2892.
[35] A. D. Bain, L. A. Cramer, *J. Magn. Reson. A* **1996**, *118*, 21.
[36] Error limits quoted are twice the standard errors estimated by cifit.
[37] A. D. Bond, J. Clayden, A. E. H. Wheatley, *Acta Crystallogr. Sect. E* **2001**, *57*, 291.

Received: September 19, 2001 [F3562]